Evolution of increased glia–neuron ratios in the human frontal cortex

Chet C. Sherwood[a,b], Cheryl D. Stimpson[a], Mary Ann Raghanti[c], Derek E. Wildman[d,e,f], Monica Uddin[d], Lawrence I. Grossman[d], Morris Goodman[b,d,g], John C. Redmond[h], Christopher J. Bonar[i], Joseph M. Erwin[j], and Patrick R. Hof[k,l]

[a]Department of Anthropology, The George Washington University, Washington, DC 20052; [c]Department of Anthropology and School of Biomedical Sciences, Kent State University, Kent, OH 44242; [d]Center for Molecular Medicine and Genetics and Departments of [g]Anatomy and Cell Biology and [f]Obstetrics and Gynecology, Wayne State University School of Medicine, Detroit, MI 48201; [e]Perinatology Research Branch, National Institute of Child Health and Human Development, National Institutes of Health, Bethesda, MD 20892; [h]Division of Neuroscience and Center for Behavioral Neuroscience, Yerkes National Primate Research Center, Emory University, Atlanta, GA 30329; [i]Cleveland Metroparks Zoo, Cleveland, OH 44109; [j]Foundation for Comparative and Conservation Biology, Needmore, PA 17238; [k]Department of Neuroscience, Mount Sinai School of Medicine, New York, NY 10029; and [l]New York Consortium in Evolutionary Primatology, New York, NY

Contributed by Morris Goodman, July 14, 2006

Evidence from comparative studies of gene expression and evolution suggest that human neocortical neurons may be characterized by unusually high levels of energy metabolism. The current study examined whether there is a disproportionate increase in glial cell density in the human frontal cortex in comparison with other anthropoid primate species (New World monkeys, Old World monkeys, and hominoids) to support greater metabolic demands. Among 18 species of anthropoids, humans displayed the greatest departure from allometric scaling expectations for the density of glia relative to neurons in layer II/III of dorsolateral prefrontal cortex (area 9L). However, the human glia–neuron ratio in this prefrontal region did not differ significantly from allometric predictions based on brain size. Further analyses of glia–neuron ratios across frontal areas 4, 9L, 32, and 44 in a sample of humans, chimpanzees, and macaque monkeys showed that regions involved in specialized human cognitive functions, such as ''theory of mind'' (area 32) and language (area 44) have not evolved differentially higher requirements for metabolic support. Taken together, these findings suggest that greater metabolic consumption of human neocortical neurons relates to the energetic costs of maintaining expansive dendritic arbors and long-range projecting axons in the context of an enlarged brain.

allometry | human evolution | prefrontal cortex | brain energy metabolism | language evolution

Humans are distinguished from other primates by a dramatically enlarged neocortex and the elaboration of cognitive capacities that have culminated in the evolution of language, technological innovation, and complex social behavior. Expansion of the human brain entails high metabolic costs (1). Although the human brain comprises only ≈2% of body mass, it captures ≈20% of the body's total glucose utilization (2). At the same time, because the metabolic rate per gram of neural tissue generally decreases with larger brain size, the human brain is more energetically efficient than that in smaller-brained primate species (3). Despite this evidence for relatively lower mass-specific brain metabolism in humans, recent microarray studies have shown that genes involved in neuronal signaling and energy production are up-regulated in the human neocortex compared with chimpanzees and other great apes (4, 5). Furthermore, evidence for positive selection in the human lineage for genes that encode components of the mitochondrial electron-transport chain suggests that there has been evolutionary pressure for high rates of aerobic energy consumption in metabolically active cells, such as neurons (6). Taken collectively, these findings suggest that neuronal activity level and energy expenditure per neuron have become enhanced in human evolution, even as mass-specific rates of brain metabolism declined. This pattern is consistent with a model that predicts that, with increases in brain size, a progressively smaller fraction of the total neuron population may be concurrently active, leading to more modularized information coding (7, 8).

An indirect measure of metabolic support supplied to neurons can be obtained by examining the ratio of glia to neurons. Glial cells, particularly astrocytes, play a crucial role in the flux of energy substrates to neurons by regulating the rate of glucose uptake and phosphorylation in response to glutamate concentrations in the synaptic cleft (9). The other main type of glial cell, oligodendrocytes, synthesize the myelin that ensheathes axons in the brain to facilitate long-range propagation of action potentials. The proliferation of both these glial cell types is responsive to trophic cues associated with neuronal activity (10–12). Thus, the local density of glia in the normal brain provides an indication of the metabolic demand of neighboring neurons. Indeed, because adult neocortical neuron numbers are attained at around the time of birth in humans, the tremendous growth of the neocortex during postnatal development is due to elaboration of dendritic arbors and a 4-fold increase in glial cell numbers (13, 14). Several experimental studies in rodents, furthermore, have demonstrated that the glia–neuron ratio increases with greater environmental enrichment and stimulation (15, 16).

Here, we investigate whether glial cell densities are relatively increased in human frontal cortex compared with other anthropoid primates (i.e., New World monkeys, Old World monkeys, and hominoids). Because the human brain is approximately three times larger than that of great apes, the increased metabolic demand of human neocortical neurons might simply be the expected allometric consequence of cell physiology associated with larger overall brain size. Alternatively, the energetic consumption of neurons in the human neocortex might exceed allometric predictions and represent a unique trait that has contributed to the evolution of human intelligence. To examine these possibilities, we tested the hypothesis that humans have disproportionately more glial cells than would be expected based on allometric scaling within a region of the dorsolateral prefrontal cortex (area 9L) that is involved in ''working memory.''

In addition, because the neocortex is functionally and architecturally heterogeneous, particular regions that subserve human cognitive specializations might display differential energetic

Conflict of interest statement: No conflicts declared.

Abbreviations: CI, confidence interval; LS, least-squares; PI, prediction interval; RMA, reduced major axis.

See Commentary on page 13563.

[b]To whom correspondence may be addressed at: Department of Anthropology, The George Washington University, 2110 G Street NW, Washington, DC 20052. E-mail: sherwood@gwu.edu or mgoodwayne@aol.com.

Table 1. Brain weights and glia–neuron ratios for layer II/III of prefrontal area 9L (species mean)

Species	*n*	Brain weight, g	Glia–neuron ratio
Homo sapiens	6	1,373.3	1.65
Pan troglodytes	6	336.2	1.20
Gorilla gorilla	2	509.2	1.21
Pongo pygmaeus	2	342.7	0.98
Hylobates muelleri	1	101.8	1.22
Papio anubis	2	155.8	0.97
Mandrillus sphinx	1	159.2	1.02
Macaca maura	6	92.6	0.84
Erythrocebus patas	2	102.3	1.09
Cercopithecus kandti	1	71.6	1.15
Colobus angolensis	1	74.4	1.20
Trachypithecus francoisi	1	91.2	1.14
Alouatta caraya	1	55.8	1.12
Saimiri boliviensis	1	24.1	0.51
Aotus trivirgatus	1	13.2	0.63
Saguinus oedipus	1	10.0	0.46
Leontopithecus rosalia	2	12.2	0.60
Pithecia pithecia	1	30.0	0.64

demands relative to other primates. Arguably, the most distinctive cognitive capacities expressed by humans are the ability to use symbolic language in a recursive manner (17) and to make inferences regarding the mental states of others, i.e., "theory of mind" (18). Area 44 in the inferior frontal cortex is considered part of Broca's area for language production (19) and the anterior paracingulate cortex (area 32) has been shown to be selectively activated in tasks that use theory of mind (20, 21). Therefore, we hypothesized that humans would differ from chimpanzees (*Pan troglodytes*) and macaque monkeys (*Macaca maura*) in displaying relatively higher glia–neuron ratios within anterior paracingulate cortex (area 32) and Broca's area (area 44) versus primary motor cortex (area 4) and dorsolateral prefrontal cortex (area 9L).

Results

The results of stereologic estimates of cell densities are shown in Table 3, which is published as supporting information on the PNAS web site. The glia–neuron ratios derived from these cell counts are presented in Table 1. We did not perform complete analyses of neuron and glial density scaling directly against brain weight because of possible artifacts related to tissue shrinkage of individual specimens in this sample; however, plots and regression exponents and a discussion of these relationships are available in Fig. 3, which is published as supporting information on the PNAS web site.

Our first analyses concerned the allometric scaling of glial cell density against neuron density in dorsolateral prefrontal cortex (area 9L) across anthropoid species (Fig. 1*A*). Glial cell density scaled against neuron density with a significant positive allometric exponent, as revealed by analysis of both species mean data [reduced major axis (RMA) slope = 1.38, lower confidence interval (CI) = 0.88, upper CI = 2.15; $r = 0.499$, $P = 0.035$] and independent contrasts (RMA slope = 1.25, $r = 0.756$, $P < 0.001$). Although human glial density was contained within the 95% prediction intervals (PIs) of the least-squares (LS) regression line of nonhuman species data (observed log glial density = 5.19; predicted = 4.94; upper PI = 5.27, lower PI = 4.60), it was the greatest positive outlier (studentized deleted residual = 1.85). Based on the nonhuman species mean LS regression, humans displayed a 46% greater density of glial cells per neuron than expected. Glial densities were predicted based on neuron density for each individual human in our sample ($n = 6$) by using the nonhuman LS regression function. As a group, the observed human glial densities were significantly greater than their paired predictions [paired samples *t* test: $t = 10.06$, degrees of freedom (df) = 5, $P < 0.001$]. Next, we used independent contrasts data to generate a LS regression line to predict glial density based on neuron density for a hypothetical species attached to the branch leading to humans in the phylogenetic tree. From this prediction, glial density in humans fell within the 95% PIs (observed log glial density = 5.19; predicted = 5.02; upper PI = 5.40, lower PI = 4.63) and represented 32% more glia than expected.

Across anthropoid primates, the RMA fit of area 9L glia–neuron ratio against brain weight (Fig. 1*B*) yielded a significant negative allometric relationship based on both species mean data (RMA slope = 0.26, lower CI = 0.20, upper CI = 0.35, $r = 0.840$, $P < 0.001$) and independent contrasts (RMA slope = 0.31, $r = 0.649$, $P = 0.004$). When the nonhuman species data were used to generate a LS regression prediction, the human value was only 5% less than expected (observed log glia–neuron ratio = 0.22; predicted = 0.23; upper PI = 0.44, lower PI = 0.03). The paired comparisons between individual observed human glia–neuron ratios and predictions based on the nonhuman LS regression line did not reveal a significant difference (paired-samples *t* test: $t = -1.10$, df = 5, $P = 0.321$). The independent contrasts prediction for glia–neuron ratio in humans based on nonhuman data showed that humans have only a 5% greater glia–neuron ratio than expected when taking phylogeny into account (observed log glia–neuron ratio = 0.22; predicted = 0.20; upper PI = 0.53, lower PI = 0.12).

Our next analyses investigated whether human glia–neuron ratios in the frontal cortex display a pattern of regional variation that differs from other primates. Individual data on glia–neuron ratios in layer II/III of areas 4, 9L, 32, and 44 in humans, chimpanzees, and macaque monkeys (Table 2) were analyzed by using repeated-measures ANOVA (Fig. 1*C*). The ANOVA revealed a significant main effect of species ($F_{2,15} = 101.80$, $P < 0.001$) and cortical area ($F_{3,45} = 22.46$, $P < 0.001$) but no interaction effect ($F_{6,45} = 1.19$, $P = 0.331$). Bonferroni post hoc comparisons showed that areas 4 and 32 differed significantly in glia–neuron ratio from one another in macaques and chimpanzees (all comparisons, $P < 0.05$). In humans, glia–neuron ratios in area 4 differed significantly from all other frontal areas (all comparisons, $P < 0.05$). Post hoc tests of homologous cortical areas among species indicated that chimpanzees and macaques did not differ significantly in glia–neuron ratios from each other. In contrast, humans had significantly greater glia–neuron ratios than macaques for every cortical area (all comparisons, $P < 0.05$) and greater glia–neuron ratios than chimpanzees in area 4 ($P < 0.05$) and area 32 ($P < 0.05$) but not area 9L ($P = 0.104$) or area 44 ($P = 1.000$).

Discussion

The human frontal cortex displays a higher ratio of glia to neurons than in other anthropoid primates. However, this relative increase in glia conforms to allometric scaling expectations, when taking into consideration the dramatic enlargement of the human brain. We suggest that relatively greater numbers of glia in the human neocortex relate to the energetic costs of maintaining larger dendritic arbors and long-range projecting axons in the context of a large brain.

Brain Size Determines Interspecific Differences in Glia–Neuron Ratio. Previous studies of glia–neuron ratios in the neocortex also concluded that brain size is the main determinant of this variable across mammals (22–24). However, these data are problematic for interpreting human brain evolution in a number of ways. First, they included relatively few species drawn from very diverse phylogenetic groups, and they represented a small number of cortical areas. Second, because scaling relationships were

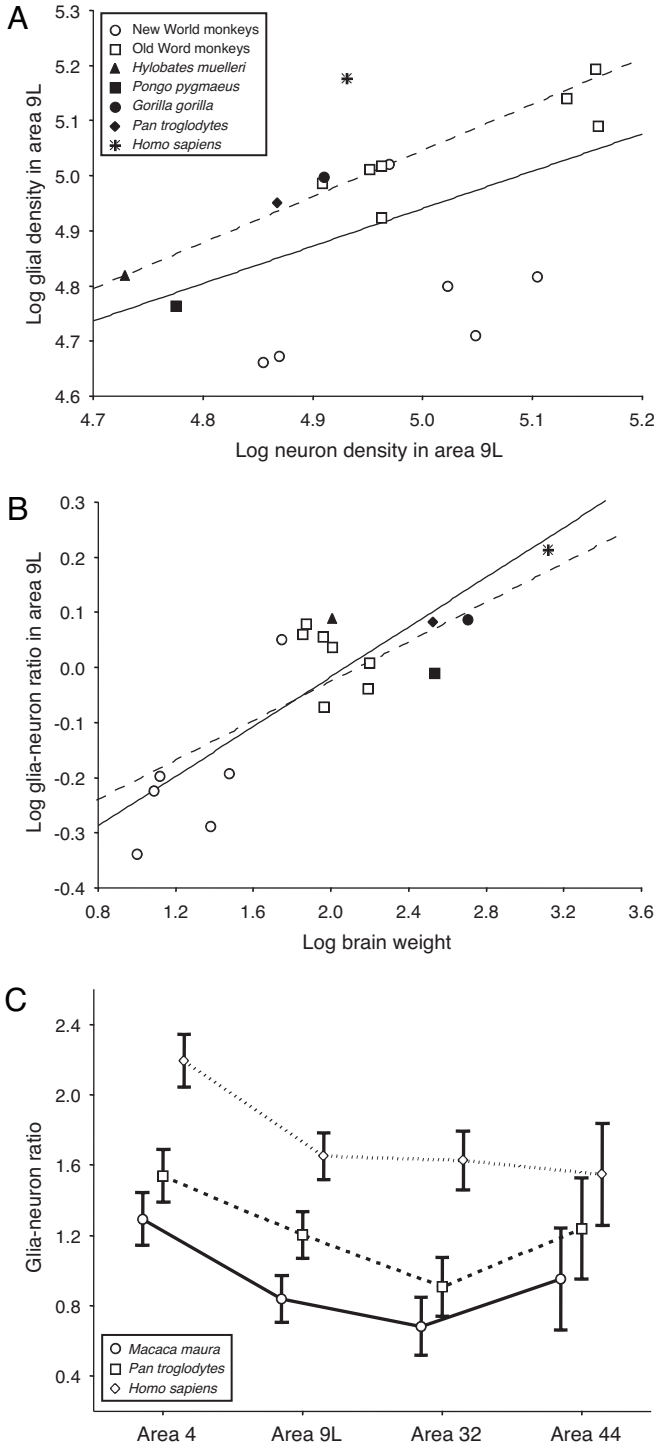

Fig. 1. Glial cell distributions in anthropoid primates. (*A*) The allometric scaling of species mean glial cell density (cells per cubed millimeter) against neuron density (cells per cubed millimeter) in layer II/III of area 9L in anthropoid primates. A solid line represents the LS regression line that is fit to the nonhuman anthropoids based on species mean data ($y = 0.68x + 1.54$; $r = 0.534$; $P = 0.027$). A dashed line represents the LS regression line that is fit to independent contrasts mapped back into ''tip'' species space, calculated to predict a hypothetical species attached to the branch leading to humans by pruning humans from the tree and rerooting it. It should be noted that absolute values for cell densities may show some error from fixation artifact; however, because each individual data point is affected by such error equally in both *x* and *y*, the slope and residuals are reliable. (*B*) The allometric scaling of the glia–neuron ratio against brain weight in layer II/III of area 9L in anthropoid primates. A solid line represents the LS regression line that is fit to the nonhuman species mean data ($y = 0.23x - 0.47$; $r = 0.804$; $P < 0.001$). A dashed line represents the LS regression line that is fit to independent contrasts mapped back into tip species space with humans pruned from the tree. (*C*) Glia–neuron ratio across frontal areas in humans, chimpanzees, and macaque monkeys ($n = 6$ for each species), showing means and 95% CIs.

Table 2. Glia–neuron ratios in layer II/III of different areas in frontal cortex

Species	*n*	Area 4	Area 9L	Area 32	Area 44
Homo sapiens	6	2.19 (0.06)	1.65 (0.09)	1.63 (0.09)	1.55 (0.18)
Pan troglodytes	6	1.54 (0.05)	1.20 (0.06)	0.91 (0.09)	1.24 (0.13)
Macaca maura	6	1.29 (0.09)	0.84 (0.03)	0.68 (0.05)	0.95 (0.06)

Data are presented as mean (standard error).

calculated based on contemporary species data, it was not clear whether these associations would be maintained after correcting for statistical nonindependence due to phylogenetic relatedness. In contrast, the current study was designed specifically to evaluate human glial densities in reference to the allometric scaling patterns in close phylogenetic relatives, other anthropoid primates. It is noteworthy that our analyses of species data and independent contrasts yielded similar allometric exponents: Independent contrast slopes were always contained within the 95% CIs of slopes calculated from species data. This finding indicates that the scaling relationships observed in contemporary taxa represent changes that have occurred repeatedly throughout multiple nodes in the phylogenetic tree and, hence, represent robust functional regularities in neocortical design.

Our results showed that area 9L of the human prefrontal cortex has higher glial density than expected for neuron density based on allometric scaling in nonhuman anthropoids, a finding that is consistent when both species mean data (46% more glia per neuron) and independent contrasts (32% more glia per neuron) are used. Additional analyses indicated that increased densities of glia relative to neurons also characterize other areas of the human frontal cortex compared with chimpanzees (areas 4 and 32) and macaque monkeys (all cortical areas examined). What might explain this relative increase in the numbers of glia in the human frontal cortex? Although only a small proportion of the variance in glial density is explained by neuron density ($r^2 = 0.25, P = 0.035$), the glia–neuron ratio is strongly associated with brain weight ($r^2 = 0.71$, $P < 0.001$). Indeed, human glia–neuron ratios did not significantly differ from nonhuman anthropoid allometric predictions based on brain weight. Mammals with even larger absolute neocortex size than humans, such as whales, are reported to have correspondingly higher glia–neuron ratios (23, 24). Taken together, these results suggest that overall brain size comprises an important factor that governs the ratio of glia to neurons.

Metabolic Correlates of Increased Glia–Neuron Ratio. The increased ratio of glia to neurons in the human frontal cortex might be explained by energy expenditures that are correlated with increasing neocortex size, which, in humans, accounts for 44% of the brain's total energy consumption (8). The two highest costs associated with neuronal activity come from excitatory postsynaptic potentials in the dendritic tree and propagation of action potentials along the axon (8). Thus, the energy required per neuron to sustain the Na^+/K^+ pumps that restore ion gradients to generate electrical potentials is expected to increase in neurons with longer dendrites and axons. Comparative studies of pyramidal neurons in granular prefrontal cortex have shown that human neurons display much larger dendritic arbors and more spines than those in primates with smaller brains (although hominoids have not yet been studied) (25).

Axon diameter and length also increase in larger brains (26), contributing to the higher cost of neuronal activity. In this context, it is interesting that glia densities have been shown to increase along different segmental levels of Clarke's nucleus surrounding neurons that have progressively longer axon projections in the spinocerebellar tract (22).

Considering the relatively greater surface area of neuronal soma, dendrites, and axons that accompany brain enlargement, it has been estimated that each human neocortical neuron consumes 3.3 times more ATP to fire a single spike than in rats, and 2.6 times more energy to maintain resting potentials (8). Accordingly, our results suggest that relatively more glia might proliferate to provide metabolic support to neurons that are increasingly energetically expensive in larger neocortices, such as in humans. In fact, certain populations of neurons that provide long corticocortical association projections linking the prefrontal cortex, temporal cortex, and parietal cortex in primates show metabolically costly characteristics, such as highly myelinated, large axons and fast firing properties (27–30). In humans, neurons in the prefrontal cortex with specialization such as these exhibit enhanced susceptibility to neurodegeneration in the course of disorders like Alzheimer's disease (31–34). These neurons may also be preferentially vulnerable to alterations of energy metabolism that occur in many age-related degenerative brain illnesses. It is, furthermore, conceivable that increased number of glia in humans may increase susceptibility to certain diseases that involve these cell types, such as schizophrenia (35).

The Correlation Between Glia–Neuron Ratio and Brain Size Corresponds to Gene Evolution. Relatively higher glia–neuron ratios in the human neocortex are most likely an epigenetic consequence of the elevated metabolic costs of maintaining membrane potentials in neurons that are situated within an enlarged brain. Hence, whenever significant evolutionary changes in brain size occur, there might be corresponding modifications to the processes underlying energy metabolism. Indeed, considerable evidence indicates that the biochemical mechanism of generating energy has been under evolutionary selection going back at least to the anthropoid primate stem, presumably to fuel increases in brain size. First, an evolutionary switch in the lactate dehydrogenase enzyme occurred among haplorhines from expression of an isozyme that predominantly supports anaerobic metabolism to one that predominantly supports oxidative metabolism (36). Lactate generated in glia, particularly astrocytes, can serve as a substrate for the oxidative metabolism of adjacent neurons (37). Second, the process of mitochondrial electron transport shows accelerated evolution of multiple subunits of complex III, complex IV, and cytochrome *c* (6, 38), suggesting that the engine of energy generation has been a prominent target of Darwinian positive selection in anthropoid primates.

Comparative microarray experiments have also revealed up-regulation of genes in the human neocortex related to energy metabolism (4, 5). For example, the gene encoding carbonic anhydrase 2, *CA2*, is up-regulated in the human cortex compared with chimpanzees and other primates (5). Carbonic anhydrases are expressed in glial cells and are involved in modulating CO_2 and other metabolic end products to levels that may enable buffering/secretion of lactate (37, 39). Given our current results, it is possible that part of the increase in transcript levels of *CA2* and other glia-expressed genes observed in the human cerebral cortex is due to relatively greater numbers of these cell types.

Regional Variation in the Glia–Neuron Ratio. Our analyses of glia–neuron ratios in functionally distinct areas of the frontal cortex (areas 4, 9L, 32, and 44) did not reveal a significant species × cortical area interaction effect in the ANOVA model, indicating that increased glia–neuron ratios in the human frontal cortex follows a pattern of regional variation that resembles both chimpanzees and macaque monkeys. This finding suggests that regional differences in the energetics of frontal cortex have been largely conserved over ≈25 million years of catarrhine evolution since the last common ancestor shared by macaques and humans. These data provide further support for the idea that human cognitive and linguistic specializations have emerged by elaborating on higher-order executive functions of the prefrontal cortex, such as planning, working memory, attention, communication, and social cognition, that evolved earlier in the primate lineage (40–42).

Conclusion

In summary, our results are consistent with the hypothesis that interspecific variation in the glia–neuron ratio in the neocortex of anthropoid primates is driven by the metabolic costs borne by single neurons in association with the energy required by larger dendritic arbors and longer axons. In this regard, human glia–neuron ratios in frontal cortex are well predicted by scaling expectations for brain size calculated from nonhuman anthropoid primates. These findings might help to explain the selection for cellular mechanisms to enhance energy metabolism that have occurred in the lineage leading to humans. This study demonstrates the potential of integrating data from histology to gain insight into the genetic changes underlying brain evolution.

Materials and Methods

Sample and Histological Preparation. The left hemisphere from postmortem brain samples representing 18 anthropoid primate species were used for these analyses (see Table 4, which is published as supporting information on the PNAS web site, for details regarding sample sizes, age, and sex characteristics). The majority of specimens came from adults, with the exception of two juveniles that had a brain size comparable with their species typical adult average (*Trachypithecus francoisi* and *Pithecia pithecia*). None of the brain samples showed evidence of neuropathological abnormality on routine examination. Many postmortem brain specimens used in this study were donated by zoological or research institutions after immersion fixation in 10% buffered formalin. Some samples were obtained from animals that were perfused transcardially with 4% paraformaldehyde in the context of unrelated experiments (*Papio anubis*, *Macaca maura*, *Erythrocebus patas*, *Saimiri boliviensis*, and *Aotus trivirgatus*). Human brain specimens from nongeriatric adults under 55 years of age were obtained from the Northwestern University Alzheimer's Disease Center Brain Bank. These specimens were immersion-fixed in 10% buffered formalin. Brain weights were recorded from each specimen and used in scaling analyses. For all nonhuman specimens, the entire frontal lobe was sectioned in the coronal plane. Human brain samples were dissected from the regions of interest as 4-cm-thick slabs. Tissue blocks were cryoprotected by immersion with increasing concentrations of sucrose solution up to 30%. Blocks were frozen on dry ice, sections were cut at 40 μm by using a sliding microtome, and a 1:10 series of sections was stained for Nissl substance with a solution of 0.5% cresyl violet. Additional details on the materials and experimental procedures can be found in *Supporting Materials and Methods*, which is published as supporting information on the PNAS web site.

Identification of Cortical Areas, Neurons, and Glia. Interspecific allometric scaling analyses used cell densities in layer II/III of dorsolateral prefrontal area 9L (Fig. 4, which is published as supporting information on the PNAS web site). Although the cytoarchitecture of area 9L has not been described for every species included in this study, reports from a diverse range of anthropoids generally agree in the location and principal cytoarchitectural features of area 9L: *Callithrix jacchus* (43), *Saimiri*

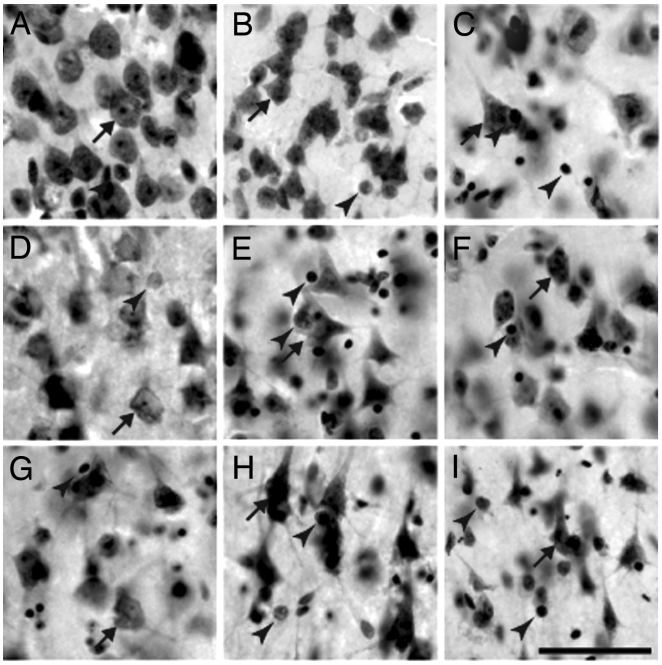

Fig. 2. Nissl staining of neurons and glia from different species in layer II/III of area 9L. Arrows indicate examples of neurons, and arrowheads indicate examples of glia. *Aotus trivirgatus* (*A*), *Saguinus oedipus* (*B*), *Alouatta caraya* (*C*), *Pithecia pithecia* (*D*), *Trachypithecus francoisi* (*E*), *Colobus angolensis* (*F*), *Cercopithecus kandti* (*G*), *Hylobates muelleri* (*H*), and *Pongo pygmaeus* (*I*). (Scale bar, 50 μm.)

oerstedii (44), *Macaca* sp. (45–47), *Papio hamadryas* (48), *Pan troglodytes* (49), and *Homo sapiens* (45, 50). Therefore, we were able to unambiguously identify this homologous cortical area across species upon histological observation, and our stereologic counts of cell densities were confined to its borders.

We performed further analyses of glia–neuron ratios in humans ($n = 6$), chimpanzees ($n = 6$), and macaque monkeys ($n = 6$) across a larger number of frontal cortical areas, including area 4 (in the region of hand representation), 9L, 32, and 44 (Fig. 5, which is published as supporting information on the PNAS web site). These regions of interest were initially identified based on topological location and confirmed by their characteristic cytoarchitecture by using descriptions from previous parcellations in these species (42, 45, 49, 51–54).

Based on Nissl-stained sections, neurons were distinguished from glia and endothelial cells by the presence of dark, coarsely stained Nissl substance in the cytoplasm, a large nucleus, a distinct nucleolus, and lightly stained proximal segments of dendritic processes (Fig. 2). In contrast, glial cells lack a conspicuous nucleolus and contain less endoplasmic reticulum. Similar to previous comparative studies of glia–neuron ratios (22, 23), we did not distinguish between astrocytes and oligodendrocytes, and microglia were excluded.

Stereologic Analyses. The optical disector method was used to calculate densities of neurons and glial cells (55). Quantification of cellular densities within layer II/III was performed by using a computerized stereology system consisting of a Zeiss (Oberkochen, Germany) Axioplan 2 photomicroscope equipped with a Ludl (Hawthorne, NY) XY motorized stage, Heidenhain (Plymouth, MN) *z*-axis encoder, an Optronics (East Muskogee, OK) MicroFire color video camera, a Dell (Round Rock, TX) PC workstation, and StereoInvestigator software (MicroBrightField, Wiliston, VT). Within each cortical area, beginning at a random starting point, three sections equidistantly spaced 400 μm apart were selected for analysis for each cell type. After outlining the boundaries of layer II/III, a set of counting frames (30×30 μm) were placed in a systematic random fashion to cover the sampled area with $\approx$30 frames per section by using a fractionator sampling design. Disector analysis was performed under Koehler illumination using a 63$\times$ objective (Zeiss Plan-Apochromat, N.A. 1.4). Each cell type was counted when its nucleolus was encountered within the counting frame. The thickness of disectors was consistently set to 6 μm to allow for a minimum 2-μm guard zone on either side of the section. On average, the coefficient of error (56) of optical disector analyses was 0.085 $\pm$ 0.018 (mean $\pm$ SD). Cellular densities (N_v) were derived from these stereologic counts and corrected for shrinkage from histological processing by the number-weighted mean section thickness as described in Sherwood *et al.* (57).

Data Analysis. Logarithmic (base 10)-transformed species means were used in allometric scaling analyses of glial cells in prefrontal area 9L. To determine the exponent of scaling relationships, we used RMA line-fitting to bivariate data because this method accounts for error in both independent and dependent variables (58). All RMA routines and tests were calculated by using (S)MATR software version 1.0 (Falster D. S., Warton, D. I., and Wright, I. J.; www.bio.mq.edu.au/ecology/SMATR). Phylogenetic independent contrasts were also calculated from the data to examine scaling relationships while controlling for the effects of phylogenetic relatedness in the data set (59). Standardized independent contrasts were calculated by using the PDAP:PDTREE module (60) of Mesquite software version 1.06 (61) from log-transformed data based on a phylogeny of primates in Goodman *et al.* (62). Branch lengths were transformed according to Pagel's method (63), which assigns all branch lengths to 1, with the constraint that tips are contemporaneous.

In addition to estimating scaling exponents, we also examined whether human glial cell densities represent significant deviations from allometric expectations based on other anthropoid primates. We calculated LS prediction equations and PIs for humans based on nonhumans using both species mean data and independent contrasts. To generate phylogenetically informed predictions based on independent contrasts, humans were pruned from the tree, the tree was rerooted so that the last common ancestor of humans and chimpanzees was at the base of the phylogeny, and then an independent contrasts regression line and prediction intervals were computed and mapped back into the original tip species space (60). After logarithmic detransformation of predictions, the percentage difference between observed and predicted values was calculated as the ratio of (observed $-$ predicted)/observed.

Differences in glia–neuron ratios among macaques, chimpanzees, and humans in different frontal cortical areas were analyzed by using a two-way ANOVA with repeated-measures design. Before these analyses, data within each group were tested for normality with the Shapiro–Wilk's W test, and homogeneity of variances was confirmed with Brown–Forsythe tests. Statistical significance level for all tests was set at $\alpha = 0.05$ (two-tailed).

We thank Drs. S. S.-H. Wang, J. K. Rilling, and M. Cáceres for providing helpful discussions and comments on an earlier version of this manuscript and E. Wahl, J. Hill, A. Zigo, A. Wolters, and K. Lever for technical assistance. This work was supported by National Science Foundation Grants BCS-0515484, BCS-0549117, and BCS-0550209; the Wenner–Gren Foundation for Anthropological Research; and James S. McDonnell Foundation Grant 22002078. Brain material used in this study was loaned by the Great Ape Aging Project, the Foundation for Comparative and Conservation Biology, the Cleveland Metroparks Zoo, the New England Primate Research Center, and the Northwestern University Alzheimer's Disease Center Brain Bank Grant P30 AG13854.

1. Aiello LC, Wheeler P (1995) *Curr Anthropol* 36:199–211.
2. Sokoloff L (1960) in *Handbook of Physiology, Section I, Neurophysiology*, eds Field J, Magoun HW, Hall VE (Am Physiol Soc, Washington, DC), Vol 3, pp 1843–1864.
3. Mink JW, Blumenschine RJ, Adams DB (1981) *Am J Physiol* 241:R203–R212.
4. Uddin M, Wildman DE, Liu G, Xu W, Johnson RM, Hof PR, Kapatos G, Grossman LI, Goodman M (2004) *Proc Natl Acad Sci USA* 101:2957–2962.
5. Cáceres M, Lachuer J, Zapala MA, Redmond JC, Kudo L, Geschwind DH, Lockhart DJ, Preuss TM, Barlow, C (2003) *Proc Natl Acad Sci USA* 100:13030–13035.
6. Grossman LI, Wildman DE, Schmidt TR, Goodman M (2004) *Trends Genet* 20:578–585.
7. Attwell D, Laughlin SB (2001) *J Cereb Blood Flow Metab* 21:1133–1145.
8. Lennie P (2003) *Curr Biol* 13:493–497.
9. Tsacopoulos M, Magistretti PJ (1996) *J Neurosci* 16:877–885.
10. Hatten ME (1985) *J Cell Biol* 100:384–396.
11. Kelic S, Levy S, Suarez C, Weinstein DE (2001) *Mol Cell Neurosci* 17:551–560.
12. Barres BA, Raff MC (1999) *J Cell Biol* 147:1123–1128.
13. Koenderink MJ, Uylings HB, Mrzljak L (1994) *Brain Res* 653:173–182.
14. Larsen CC, Bonde Larsen K, Bogdanovic N, Laursen H, Graem N, Badsberg Samuelsen G, Pakkenberg B (2006) *Neuroscience* 139:999–1003.
15. Diamond MC, Krech D, Rosenzweig MR (1964) *J Comp Neurol* 123:111–120.
16. Szeligo F, Leblond CP (1977) *J Comp Neurol* 172:247–263.
17. Hauser MD, Chomsky N, Fitch WT (2002) *Science* 298:1569–1579.
18. Tomasello M, Call J, Hare B (2003) *Trends Cogn Sci* 7:153–156.
19. Bookheimer S (2002) *Annu Rev Neurosci* 25:151–88.
20. Gallagher HL, Frith CD (2003) *Trends Cogn Sci* 7:77–83.
21. Frith CD, Frith U (2006) *Neuron* 50:531–534.
22. Friede RL, Van Houten WH (1962) *Proc Natl Acad Sci USA* 48:817–821.
23. Hawkins A, Olszewski J (1957) *Science* 126:76–77.
24. Tower DB, Young OM (1973) *J Neurochem* 20:269–278.
25. Elston GN, Benavides-Piccione R, Elston A, Zietsch B, DeFelipe J, Manger P, Casagrande V, Kaas JH (2006) *Anat Rec* 288:A26–A35.
26. Harrison KH, Hof PR, Wang SS (2002) *J Neurocytol* 31:289–298.
27. Hof PR, Nimchinsky EA, Morrison JH (1995) *J Comp Neurol* 362:109–133.
28. Hof PR, Ungerleider LG, Webster MJ, Gattass R, Adams MM, Sailstad CA, Morrison JH (1996) *J Comp Neurol* 376:112–127.
29. Fries W, Keizer K, Kuypers HG (1985) *Exp Brain Res* 58:613–616.
30. Raiguel SE, Lagae L, Gulyas B, Orban GA (1989) *Brain Res* 493:155–159.
31. Hof PR, Morrison JH (2004) *Trends Neurosci* 27:607–613.
32. Bussière T, Giannakopoulos P, Bouras C, Perl DP, Morrison JH, Hof PR (2003) *J Comp Neurol* 463:281–302.
33. Hof PR, Cox K, Morrison JH (1990) *J Comp Neurol* 301:44–54.
34. Hof PR, Morrison JH (1990) *J Comp Neurol* 301:55–64.
35. Davis KL, Stewart DG, Friedman JI, Buchsbaum M, Harvey PD, Hof PR, Buxbaum J, Haroutunian V (2003) *Arch Gen Psychiatry* 60:443–456.
36. Syner FN, Goodman M (1966) *Nature* 209:426–428.
37. Ames A, III (2000) *Brain Res Rev* 34:42–68.
38. Grossman LI, Schmidt TR, Wildman DE, Goodman M (2001) *Mol Phylogenet Evol* 18:26–36.
39. Deitmer JW (2002) *J Neurochem* 80:721–726.
40. Holloway RL (1967) *Gen Syst* 12:3–19.
41. Deacon TW (1997) *The Symbolic Species: The Co-Evolution of Language and the Brain* (Norton, New York).
42. Petrides M, Cadoret G, Mackey S (2005) *Nature* 435:1235–1238.
43. Burman KJ, Palmer SM, Gamberini M, Rosa MG (2006) *J Comp Neurol* 495:149–172.
44. Rosabal F (1967) *J Comp Neurol* 130:87–108.
45. Petrides M, Pandya DN (1999) *Eur J Neurosci* 11:1011–1036.
46. von Bonin G, Bailey P (1947) *The Neocortex of Macaca mulatta* (Univ of Illinois Press, Urbana, IL).
47. Walker AE (1940) *J Comp Neurol* 73:59–86.
48. Watanabe-Sawaguchi K, Kubota K, Arikuni T (1991) *J Comp Neurol* 311:108–133.
49. Bailey P, von Bonin G, McCulloch WS (1950) *The Isocortex of the Chimpanzee* (Univ of Illinois Press, Urbana, IL).
50. Rajkowska G, Goldman-Rakic PS (1995) *Cereb Cortex* 5:307–322.
51. Sherwood CC, Holloway RL, Erwin JM, Schleicher A, Zilles K, Hof PR (2004) *Brain Behav Evol* 63:61–81.
52. Sherwood CC, Broadfield DC, Holloway RL, Gannon PJ, Hof PR (2003) *Anat Rec* 271:A276–A285.
53. Paxinos G, Huang XF, Toga AW (2000) *The Rhesus Monkey Brain in Stereotaxic Coordinates* (Academic, San Diego).
54. Vogt BA, Nimchinsky EA, Vogt LJ, Hof PR (1995) *J Comp Neurol* 359:490–506.
55. Mouton PR (2002) *Principles and Practices of Unbiased Stereology: An Introduction for Bioscientists* (The Johns Hopkins Univ Press, Baltimore).
56. Schmitz C, Hof PR (2000) *J Chem Neuroanat* 20:93–114.
57. Sherwood CC, Raghanti MA, Stimpson CD, Bonar CJ, de Sousa AA, Preuss TM, Hof PR *Brain Behav Evol*, in press.
58. Sokal RR, Rohlf FJ (1995) *Biometry: The Principles and Practice of Statistics in Biological Research* (Freeman, San Francisco).
59. Felsenstein J (1985) *Am Nat* 125:1–15.
60. Garland T, Ives AR (2000) *Am Nat* 155:346–364.
61. Maddison WP, Maddison DR (2005) *Mesquite: A Modular System for Evolutionary Analysis*, Ver 1.06, http://mesquiteproject.org.
62. Goodman M, Grossman LI, Wildman DE (2005) *Trends Genet* 21:511–517.
63. Pagel MD (1992) *J Theor Biol* 156:431–442.